α-L-LNA (α-L-*ribo* Configured Locked Nucleic Acid) Recognition of DNA: An NMR Spectroscopic Study

Katrine M. Ellemann Nielsen,[a] Michael Petersen,*[a] Anders E. Håkansson,[b] Jesper Wengel,[a] and Jens Peter Jacobsen[a]

Abstract: We have used NMR and CD spectroscopy to study and characterise two α-L-LNA:DNA duplexes, a nonamer that incorporates three α-L-LNA nucleotides and a decamer that incorporates four α-L-LNA nucleotides, in which α-L-LNA is α-L-*ribo*-configured locked nucleic acid. Both duplexes adopt right-handed helical conformations and form normal Watson–Crick base pairing with all nucleobases in the *anti* conformation. Deoxyribose conformations were determined from measurements of scalar coupling constants in the sugar rings, and for the decamer duplex, distance information was derived from $^1H-^1H$ NOE measurements. In general, the deoxyriboses in both of the α-L-LNA:DNA duplexes adopt *S*-type (B-type structure) sugar puckers, that is the inclusion of the modified α-L-LNA nucleotides does not perturb the local native B-like double-stranded DNA (dsDNA) structure. The CD spectra of the duplexes confirm these findings, as these display B-type characteristic features that allow us to characterise the overall duplex type as B-like. The $^1H-^1H$ NOE distances which were determined for the decamer duplex were employed in a simulated annealing protocol to generate a model structure for this duplex, thus allowing a more detailed inspection of the impact of the α-L-*ribo*-configured nucleotides. In this structure, it is evident that the malleable DNA backbone rearranges in the vicinity of the modified nucleotides in order to accommodate them and present their nucleobases in a geometry suitable for Watson–Crick base pairing.

Keywords: DNA · DNA structures · LNA · NMR spectroscopy · oligonucleotides

Introduction

The ideal antisense gene inhibitor should display high affinity and selectivity towards its target sequence, enhanced stability towards intra- and extracellular nucleases, and be able to penetrate the cell membrane. In addition to these requirements, the ideal antisense oligonucleotide (AO) should leave the nucleic acid structure relatively unperturbed in order to retain the ability to elicit RNase H degradation of the resulting AO:RNA hybrid. Natural unmodified oligonucleotides meet some of these requirements but are unstable in the cellular environment. Thus, an extensive research in chemically modified nucleotides has been prompted and many chemical modifications in either the phosphate linker, the nucleobase, or the sugar ring have been synthesised and tested.[1] As yet, only a few of this plethora of nucleic acid analogues have been found to possess the ability to invoke RNase H degradation of their cognate RNA, for example phosphorothioates,[2] phosphorodithioates,[3] arabinonucleic acids,[4] and cyclohexenyl nucleic acids.[5, 6]

Recently, the nucleic acid analogue, LNA (Locked Nucleic Acid; Scheme 1), has been introduced.[7–9] An LNA nucleotide contains a 2′-*O*,4′-*C*-methylene bridge that locks the nucleotide in a C3′-*endo* (*N*-type) furanose conformation. Oligonucleotides which contain one or more LNA nucleotides have displayed a number of appealing features, for example unprecedented thermal affinities when hybridised with both complementary DNA or RNA, with increases in melting temperatures up to +9.6 °C per modification,[7–10] stability in serum, the ability to be transported into living cells, and the ability to activate *E. coli* RNase H, both as LNA/DNA gapmers and mixmers when hybridised with cognate RNA, albeit at significantly slower rates in the case of the mixmers.[11]

[a] Dr. M. Petersen, K. M. E. Nielsen, Prof. J. Wengel, Prof. J. P. Jacobsen
Nucleic Acid Center,[+] Department of Chemistry
University of Southern Denmark, Odense University
5230 Odense M (Denmark)
Fax: (+45) 66-158-780
E-mail: mip@chem.sdu.dk

[b] A. E. Håkansson
Department of Chemistry, University of Copenhagen
2100 Copenhagen (Denmark)

[+] The Nucleic Acid Center is funded by the Danish National Research Foundation for studies on the chemical biology of nucleic acids.

Supporting information for this article is available on the WWW under http://www.chemeurj.org/ or from the author. α-L-LNA atomic charges and atom types (one page).

  0947-6539/02/0813-3001 $ 20.00+.50/0

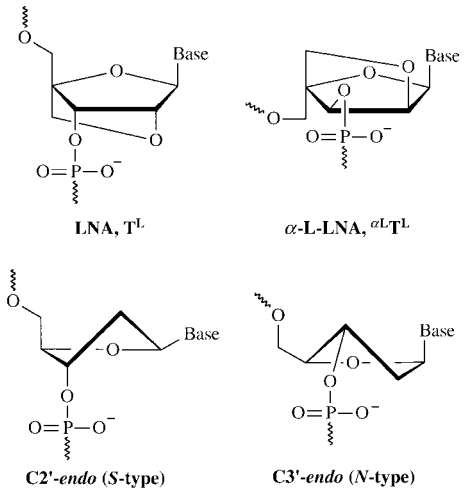

Scheme 1. The chemical structure of LNA and α-L-LNA plus C2′-*endo* and C3′-*endo* sugar conformations.

We have investigated the remarkable stability of LNA modified duplexes using NMR spectroscopy in structural studies of a number of LNA:DNA and LNA:RNA hybrids.[10, 12–16] These studies have included analysis of sugar conformations, which give information on local perturbations that are introduced by the LNA nucleotides and a gross view of the duplex structure, and determination of high-resolution solution structures. Generally, we have found that the incorporation of a single LNA nucleotide introduces local perturbations only, and that the 3′-positioned nucleotides are more perturbed than the 5′-positioned nucleotides. When LNA nucleotides are incorporated several times in duplexes, they change the overall duplex geometry towards A-type. Specifically, the high-resolution structure of a nonamer LNA:RNA hybrid with three LNA nucleotides in the LNA strand revealed an almost canonical A-type geometry of this hybrid.[16] The introduction of an A-like geometry of LNA:RNA hybrids may be responsible for the significant deterioration in RNase H activity of LNA/DNA mixmers in comparison to LNA/DNA gapmers.[11]

Recently, we have introduced a diastereoisomeric form of LNA, α-L-LNA (α-L-*ribo* configured LNA, $^{\alpha L}\mathbf{T}^{\mathbf{L}}$; Scheme 1).[17–19] Thermal affinity studies of oligonucleotides which contain this modified nucleotide have demonstrated the strong binding affinity of α-L-LNA towards both RNA and DNA with increases in melting temperature per modification of up to 5.3 °C and 4.8 °C in the cases of RNA and DNA, respectively.[17–19] The 2′-*O*,4′-*C*-methylene bridge locks the α-L-LNA sugar ring into a C3′-*endo* conformation ($_3$E, *N*-type). However, as α-L-LNA is an L-*ribo* configured nucleotide, comparison with D-*ribo* configured nucleotides at the monomer level is difficult and gives no indication of the features when built into oligonucleotides.

In order to further characterise the structural properties of duplexes containing α-L-LNA nucleotides, we have investigated two α-L-LNA:DNA duplexes using a combination of CD and NMR spectroscopy (the base sequences and numbering schemes for the two duplexes are shown in Scheme 2). The CD spectra afford a general characterisation of the overall

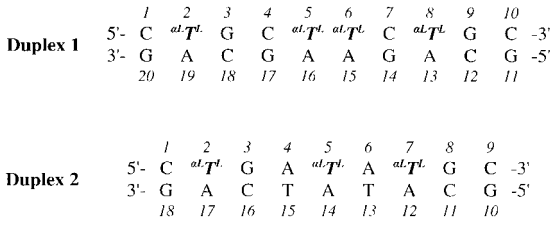

Scheme 2. Numbering scheme for the two α-L-LNA:DNA duplexes studied. $^{\alpha L}\mathbf{T}^{\mathbf{L}}$ denotes α-L-LNA modified thymidines.

duplex conformations, while measurements of the *J* coupling constants in the sugar rings by NMR spectroscopy can determine the sugar puckers of individual nucleotides in order to assess local duplex conformations. Finally, to derive a more detailed three-dimensional picture of an α-L-LNA:DNA duplex we have produced a model structure of one of the duplexes included in this study. This structure was determined from interproton distances determined from a NOESY spectrum with a mixing time of 100 ms.

Results

Thermal stabilities: The thermal stabilities of the modified α-L-LNA:DNA duplexes **1** and **2** (see Scheme 2) were determined and compared to those of the unmodified reference sequences (Table 1). Sharp monophasic transitions were obtained with hypochromicities of 1.1 – 1.2. No indications of biphasic transitions were detected. For duplex **1** and **2** we observed increases in the melting temperatures of +13.1 and +8.2 °C, respectively, relative to the unmodified dsDNA duplexes. These results emphasize the substantial increases in thermal stability displayed by α-L-LNA modified oligonucleotides when hybridised with complementary DNA.

Table 1. Melting temperatures of α-L-LNA:DNA duplexes compared with the unmodified duplexes of identical base sequence.[a]

Duplex	Duplex type	T_m [°C]	ΔT_m per mod. [°C]
1	dsDNA	33.6	–
	α-L-LNA:DNA	46.7	3.3
2	dsDNA	28.0	–
	α-L-LNA:DNA	36.2	2.7

[a] T_m is the melting temperature and ΔT_m per mod. the increase in melting temperature per α-L-LNA modified nucleotide compared with that of the corresponding unmodified dsDNA duplex.

CD spectra: The CD spectra of the two α-L-LNA:DNA duplexes are shown in Figure 1. The unmodified dsDNA version of duplex **2** and the LNA:DNA version of duplex **1**, that is the duplex with LNA nucleotides rather than α-L-LNA nucleotides at identical positions, are included in Figure 1 for comparison. The unmodified dsDNA duplex shows all the characteristics of a B-type duplex, that is no negative band at ≈210 nm, a negative band at ≈250 nm and a positive band with an approximately equal magnitude at ≈275 nm. The LNA modified duplex, on the contrary, exhibits increased A-type duplex characteristics with a fairly intense negative

  0947-6539/02/0813-3002 $ 20.00+.50/0 *Chem. Eur. J.* **2002**, *8*, No. 13

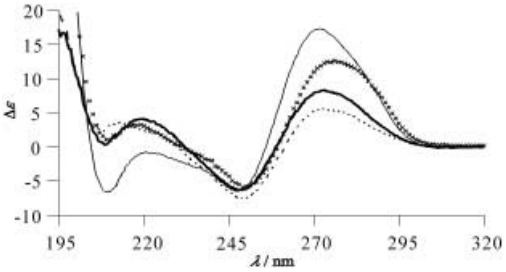

Figure 1. The CD spectra of duplex **1** (× ××), duplex **2** (——), the LNA version of duplex **1** (——), and the unmodified version of duplex **2** (- - - -).

band at ≈210 nm and a positive band at 272 nm which is of a greater magnitude than the negative band at 250 nm. This is in perfect agreement with our previous structural investigations as these studies demonstrated that this duplex possesses a conformation in-between A- and B-type.[14] Both α-L-LNA duplexes display features indicative of an overall B-type helical conformation, that is no negative band at ≈210 nm, a negative band at ≈250 nm and a positive band at ≈275 nm with approximately equal intensity. In particular, the CD spectra of the unmodified and the α-L-LNA modified versions of duplex **2** are very similar, and this indicates that the B-type appearance of this duplex[15] is retained upon introduction of the α-L-LNA nucleotides.

NMR spectroscopy: The one-dimensional ^{1}H NMR spectrum of the decamer α-L-LNA:DNA duplex (duplex **1**) only shows lines from the expected α-L-LNA:DNA duplex at 25 °C. No signs of alternative hybridisation were observed. On the other hand, the one-dimensional ^{1}H NMR spectrum of the nonamer α-L-LNA:DNA duplex (duplex **2**) at 25 °C exhibited weak lines in addition to those expected for the α-L-LNA:DNA duplex. These lines could stem from traces of single-stranded DNA or α-L-LNA or possibly from traces of a non-complementary alternative sequences. The NOESY spectra of both the duplexes display the characteristic connectivities of right-handed dsDNA duplexes with all nucleobases in the *anti* conformation. Assignment of non-exchangeable protons was performed using standard methods.[20–23] The NOESY spectra with short mixing times (50 or 100 ms) allowed unambiguous assignments of the H2′ and H2″ resonances. The H6′ and H6″ resonances in the 2′-*O*,4′-*C*-methylene bridge of the α-L-LNA nucleotides were assigned by their strong intranucleotide cross peaks to the aromatic protons of the modified nucleotides; H6′ was assigned as the proton located closer to the aromatic proton. The aromatic to H1′ region of the 100 ms NOESY spectrum of duplex **1** is shown in Figure 2. The NOESY spectra acquired in H_2O exhibit normal Watson–Crick connectivities and were employed in the assignment of the exchangeable protons. Selections of chemical shift values for the decamer and the nonamer α-L-LNA:DNA duplexes are given in Tables 2 and 3, respectively.

Sugar ring conformations: In Figure 3, a comparison between the experimental double-quantum filtered correlation spectroscopy (DQF-COSY) spectrum and the spectrum obtained by spectral simulations with CHEOPS is shown for duplex **1**. Excellent agreement between the simulated and the experimental spectrum is observed. The simulated DQF-COSY spectrum of duplex **2** also agrees well with the experimental as the spectrum shown in Figure 3. The coupling constants returned by CHEOPS were used as input for our randomised version of PSEUROT,[13] with the uncertainties of the coupling constants being gauged by monitoring the dependence of the simulation procedure on alterations in the input parameters. The coupling constants, molar fractions of *S*-type sugar conformations and pseudorotation angles of the two α-L-LNA:DNA duplexes are given in Tables 4 and 5.

Both duplexes display predominantly *S*-type sugar conformations, with populations of *S*-type conformations that generally exceed 90%, except for the two 3′-terminal nucleotides in the α-L-LNA strands. These nucleotides possess a substantial population of *N*-type sugar conformation. As shown by Tables 4 and 5, similar scenarios are observed in the duplexes, in which the penultimate nucleotides, G8 or G9,

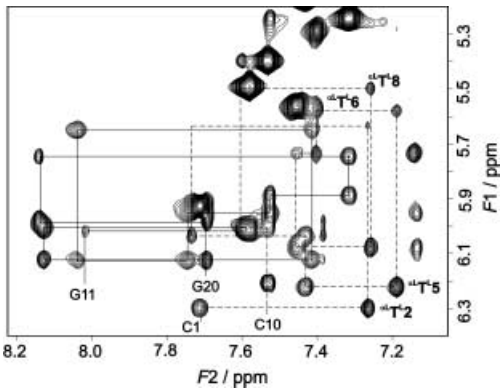

Figure 2. The aromatic–H1′ region of the 100 ms NOESY spectrum of duplex **1**. The sequential H1′($n-1$)–H6/8(n)–H1′(n) connectivity pathways are indicated; α-L-LNA strand (- - - -), DNA strand (——).

Table 2. A selection of chemical shifts (in ppm) for d(C$^{\alpha L}$**T**^{L}GC$^{\alpha L}$**T**$^{L\alpha L}$**T**^{L}-C$^{\alpha L}$**T**^{L}GC):d(GCAGAAGCAG). Values are given at 25 °C relative to DSS.[a]

	H1′	H2′	H2″	H3′	H6/H8	H5/H2/CH$_3$	H1/H3
C1	6.30	2.25	2.84	4.84	7.71	5.92	–
$^{\alpha L}$**T**^{L}**2**	5.64	4.74	–	4.74	7.27	1.73	
G3	6.03	2.38	2.70	4.73	7.74	–	12.61
C4	6.22	2.22	2.78	4.97	7.43	5.17	–
$^{\alpha L}$**T**^{L}**5**	5.58	5.29	–	4.71	7.19	1.61	14.13
$^{\alpha L}$**T**^{L}**6**	5.73	4.86	–	4.83	7.40	1.60	13.88
C7	6.08	2.30	2.78	4.65	7.45	5.56	–
$^{\alpha L}$**T**^{L}**8**	5.49	4.94	–	4.74	7.26	1.67	13.64
G9	6.01	2.29	2.60	4.51	7.60	–	12.68
C10	6.21	2.14	2.22	4.48	7.53	5.40	–
G11	6.02	2.69	2.81	4.86	8.02	–	
C12	6.01	2.37	2.67	4.90	7.58	5.49	–
A13	6.12	2.67	2.87	5.02	8.13	6.99	–
G14	5.65	2.47	2.69	4.96	7.43	–	12.22
A15	6.12	2.69	2.95	5.03	8.04	7.13	–
A16	5.94	2.52	2.68	4.97	7.75	7.14	–
G17	5.89	2.46	2.66	4.92	7.52	–	12.57
C18	5.74	2.06	2.43	4.84	7.32	5.24	–
A19	5.99	2.62	2.77	4.99	8.14	7.38	–
G20	6.12	2.44	2.29	4.62	7.70	–	

[a] The protons in the C2′,C4′ linker have the following chemical shift values: $^{\alpha L}$**T**^{L}**2** H6′/H6″: 4.30/4.41; $^{\alpha L}$**T**^{L}**5** H6′/H6″: 4.26/4.38; $^{\alpha L}$**T**^{L}**6** H6′/H6″: 4.13/4.20; $^{\alpha L}$**T**^{L}**8** H6′/H6″: 4.28/4.32.

Table 3. A selection of chemical shifts (in ppm) for d(C$^{\alpha L}$T^{L}GA$^{\alpha L}$T^{L}-A$^{\alpha L}$T^{L}GC):d(GCATATCAG). Values are given at 25°C relative to DSS.[a]

	H1′	H2′	H2″	H3′	H6/H8	H5/H2/CH$_3$	H1/H3
C1	6.29	2.22	2.81	4.84	7.71	5.93	–
$^{\alpha L}$T^{L}**2**	5.61	4.52	–	4.72	7.23	1.73	
G3	5.81	2.37	2.71	4.81	7.74	–	12.35
A4	6.33	2.76	3.07	5.12	8.30	7.76	–
$^{\alpha L}$T^{L}**5**	5.40	4.64	–	4.79	6.83	1.55	13.57
A6	6.24	2.56	2.98	4.82	8.03	7.19	–
$^{\alpha L}$T^{L}**7**	5.43	4.88	–	4.78	6.84	1.44	13.45
G8	6.01	2.28	2.60	4.49	7.49	–	12.56
C9	6.24	2.15	2.22	4.47	7.52	5.36	–
G10	6.03	2.71	2.82	4.86	8.01	–	
C11	6.07	2.47	2.65	4.90	7.59	5.50	–
A12	6.25	2.59	2.89	4.90	8.11	7.28	–
T13	5.96	2.32	2.65	4.90	7.30	1.23	12.84
A14	6.19	2.52	2.83	4.92	8.12	6.95	–
T15	5.98	2.06	2.47	4.84	7.22	1.11	13.29
C16	5.70	2.11	2.43	4.86	7.53	5.66	–
A17	5.95	2.65	2.76	5.00	8.18	7.37	–
G18	6.11	2.43	2.29	4.62	7.71	–	

[a] The protons in the C2′,C4′ linker have the following chemical shift values: $^{\alpha L}$T^{L}**2** H6′/H6″: 4.29/4.40; $^{\alpha L}$T^{L}**5** H6′/H6″: 4.32/4.32; $^{\alpha L}$T^{L}**7** H6′/H6″: 4.25/4.25.

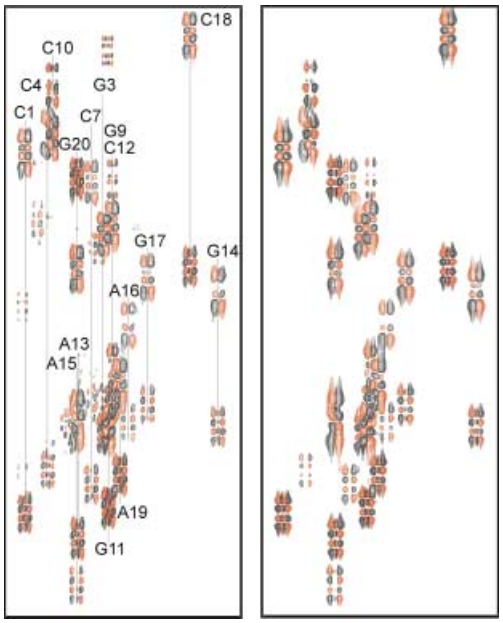

Figure 3. Comparison of the H1′–H2′/H2″ regions of the experimental (left) and the calculated (right) DQF-COSY spectra for duplex **1**.

possess ≈60% *N*-type conformation, and the terminal nucleotides, C9 or C10, ≈40% *N*-type conformation. We note that the 5′-$^{\alpha L}$T^{L}pGpC–3′ stretch is common to the two α-L-LNA strands, however, a specific 5′-$^{\alpha L}$T^{L}pG–3′ effect can be excluded since G3 in both duplexes has sugar conformations like most other nucleotides in the duplexes, that is above 90% *S*-type. An explanation for the observed phenomenon is currently unavailable but it may be attributed to increased dynamical behaviour towards these ends of the duplexes.

Model structure: As suggested by the CD spectra and from the investigation of the deoxyribose conformations in duplex **1**, this duplex possesses an overall B-type structure. To further evaluate the impact of α-L-LNA nucleotides on the structure of a dsDNA duplex, a model structure of duplex **1** was generated starting from a canonical B-type dsDNA duplex (see the Experimental Section). A total of 20 final structures were calculated using the protocol described by randomly varying the initial atomic velocities. The average pairwise all-atomic RMSD for the 20 structures was 0.78 Å for

Table 4. Coupling constants for the sugar protons in the d(C$^{\alpha L}$T^{L}GC$^{\alpha L}$T^{L}A$^{\alpha L}$T^{L}-C$^{\alpha L}$T^{L}GC):d(GCAGAAGCAG) duplex and the sugar conformations derived.[a]

	$J_{1',2'}$ [Hz]	$J_{1',2''}$ [Hz]	$J_{2',3'}$ [Hz]	$J_{2'',3'}$ [Hz]	% *S*[c]	P_N [°][d]	P_S [°][e]
C1	9.6	5.3	3.5	–0.3	97 (8)		173 (15)
$^{\alpha L}$T^{L}**2**[b]							
G3	7.4	5.2	3.7	0.0	91 (13)		186 (20)
C4	8.1	3.7	4.8	0.0	91 (12)		164 (21)
$^{\alpha L}$T^{L}**5**[b]							
$^{\alpha L}$T^{L}**6**[b]							
C7	6.9	5.3	4.7	0.0	82 (16)		176 (25)
$^{\alpha L}$T^{L}**8**[b]							
G9	3.9	7.0	5.3	6.1	41 (7)	–3 (17)	191 (25)
C10	5.9	7.0	5.9	2.9	64 (13)	18 (50)	173 (42)
G11	8.6	5.4	2.3	0.0	96 (9)		183 (15)
C12	8.1	5.6	4.4	0.1	92 (12)		182 (19)
A13	8.0	6.0	4.3	1.1	87 (12)		179 (25)
G14	9.0	5.2	4.8	0.0	92 (11)		166 (19)
A15	8.8	5.6	4.6	0.5	90 (11)		170 (21)
A16	7.8	5.4	4.8	0.0	86 (15)		172 (26)
G17	8.3	5.5	4.4	0.1	93 (12)		182 (17)
C18	8.4	6.0	3.6	0.1	97 (8)		190 (10)
A19	8.5	5.5	4.2	0.5	91 (10)		180 (15)
G20	8.1	6.1	4.6	0.0	92 (12)		178 (28)

[a] The coupling constants were derived from the H1′–H2′ and H1′–H2″ cross peaks in the selective DQF-COSY spectrum using CHEOPS. The $J_{2',2''}$ coupling constants returned were between –14.0 and –15.8 Hz, values typical for deoxyribose. The sugar conformations were calculated using a randomised version of the PSEUROT program. In PSEUROT calculations, the puckering amplitudes were fixed at 38°. The standard deviations are given in brackets. [b] The α-L-LNA nucleotides were not included in the CHEOPS calculations due to the locked conformation. [c] Percent *S*-type sugar conformation calculated using PSEUROT. [d] Pseudorotation angle calculated for the *N*-type sugar conformation. If the mol fraction of the *N*-type conformer was calculated to be below 20%, the *P* value was not considered to be determined with sufficient accuracy. [e] Pseudorotation angle calculated for the *S*-type sugar conformation.

Table 5. Coupling constants for the sugar protons in the d(C$^{\alpha L}$T^{L}GA$^{\alpha L}$T^{L}-A$^{\alpha L}$T^{L}GC):d(GCATATCAG) duplex and the derived sugar conformations.[a]

	$J_{1',2'}$ [Hz]	$J_{1'2''}$ [Hz]	$J_{2'3'}$ [Hz]	$J_{2'',3'}$ [Hz]	% *S*[c]	P_N [°][d]	P_S[°][e]
C1	9.0	5.4	3.9	0.7	92 (10)		175 (15)
$^{\alpha L}$T^{L}**2**[b]							
G3	9.1	5.6	1.8	0.0	97 (7)		182 (11)
A4	10.1	4.9	4.9	–0.4	97 (7)		154 (14)
$^{\alpha L}$T^{L}**5**[b]							
A6	7.8	5.3	3.5	–0.1	90 (12)		184 (17)
$^{\alpha L}$T^{L}**7**[b]							
G8	4.0	7.0	5.9	6.3	38 (7)	–1 (24)	179 (35)
C9	5.9	6.8	6.1	3.2	61 (9)	4 (43)	168 (39)
G10	7.8	5.5	2.1	–0.1	95 (9)		189 (12)
C11	8.4	5.2	4.1	0.0	90 (12)		172 (22)
A12	5.9	6.2	4.0	–0.2	88 (14)		192 (31)
T13	8.0	5.5	4.0	0.1	90 (12)		181 (19)
A14	7.2	6.2	4.6	–0.1	90 (14)		187 (27)
T15	8.2	6.2	3.3	0.1	97 (7)		192 (11)
C16	8.3	6.0	3.7	0.2	94 (10)		185 (18)
A17	8.7	5.8	5.0	–0.1	93 (12)		173 (25)
G18	8.6	5.9	4.7	0.1	92 (12)		179 (22)

[a]–[e] See Table 4.

0947-6539/02/0813-3004 $ 20.00+.50/0 *Chem. Eur. J.* **2002**, *8*, No. 13

all non-terminal base pairs. The largest violation observed was 0.36 Å; only 7 or 8 violations in excess of 0.2 Å were observed. The model structure was validated by calculating 20 structures from A-type starting geometry. Of these structures, 15 converged to one family of structures, while the five outliers displayed high force field and constraint energies. The RMSD for non-terminal base pairs for the 35 structures (20 from B-type starting geometry and 15 from A-type) was 1.07 Å, which shows that identical structures were obtained from either type of starting geometry. A superposition of the 20 structures calculated from B-type starting geometry is presented in Figure 4.

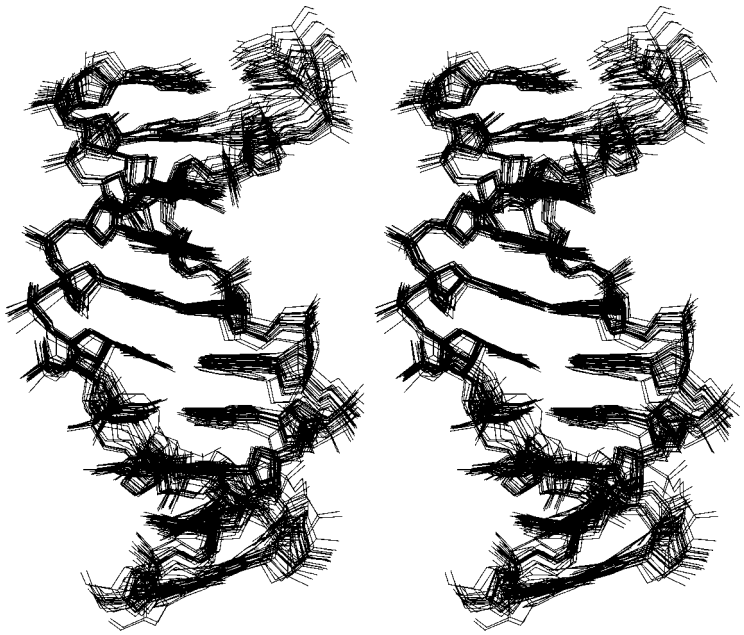

Figure 4. Stereoview of a superposition of the 20 structures calculated for duplex **1**. For clarity, hydrogens are not shown.

At a first glance, the model of duplex **1** has the overall appearance of a B-type duplex, for example the minor groove is narrow and rather deep and the base pairs pierce the long axis of the helix. The 2′-*O*,4′-*C*-methylene linkers of the α-L-LNA nucleotides are positioned at the brim of the major groove. Therefore, the modifications pose no steric hindrance in the duplex formation with complementary nucleic acids. In Figure 5, a view of the central four base pairs seen from the major groove is presented showing the positions of the modifications.

A more thorough characterisation and discussion of the model structure is given below, in which the anomalies that were introduced in the B-DNA framework by the α-L-LNA nucleotides are emphasized.

Helix parameters: The global helix axis and helical parameters were calculated with the program CURVES 5.2.[24, 25] The global helix axis is fairly straight with a slight bend at the C4:G17 base pair. Thus, the overall geometry of the α-L-LNA:DNA duplex is regular and no global incoherence is introduced by the modified nucleotides.

A selection of helical parameters for the model structure is shown in Figure 6. *X* displacement, *Y* displacement, inclination, and tip are the helix parameters with which the global helix axis is determined. These parameters then allow a direct comparison between different duplex forms and the model structure determined. We observe that the values for *X* displacement and inclination are near the values expected for a B-type duplex. *Y* displacement and tip do not discriminate between A- and B-form duplexes and merely serve as to describe the regularity of the duplex; although there are some changes along the duplex (up to ≈0.4 Å for *Y* displacement and up to ≈7° for tip), these values indicate that the duplex is fairly regular.

The value of rise is significantly different in A- and B-type DNA, with values of 2.6 and 3.4 Å, respectively. Rise in the model structure is generally close to the value for B-type DNA with an average of 3.5 Å. Some variations occur along the duplex: The T5pT6:A15pA16 base pair step has a value as low as 2.8 Å because T6 unstacks from C7 hence creating an interruption in the stacking arrangement in the α-L-LNA strand. Twist is rather poorly determined in NMR-derived structures, and the variations along the duplex cannot be attributed to the modified α-L-LNA nucleotides.

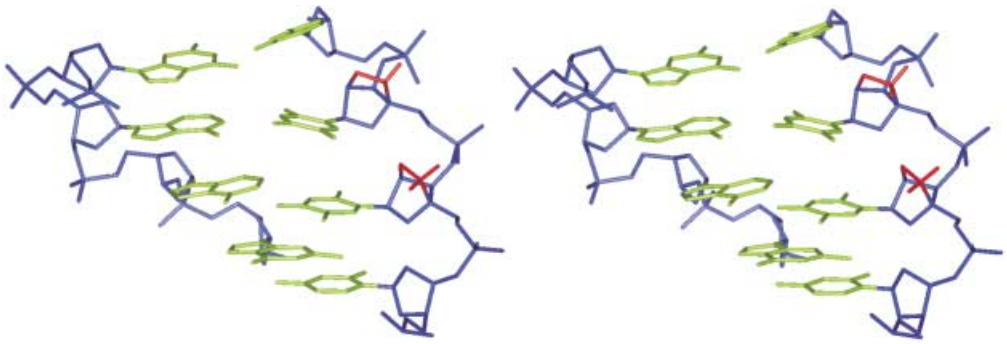

Figure 5. A view into the major groove of duplex **1** showing the central four base pairs. The colouring scheme used is: sugar-phosphate backbone: blue; nucleobases: green; the α-L-LNA 2′-*O*,4′-*C*-methylene bridge: red.

  0947-6539/02/0813-3005 $ 20.00+.50/0

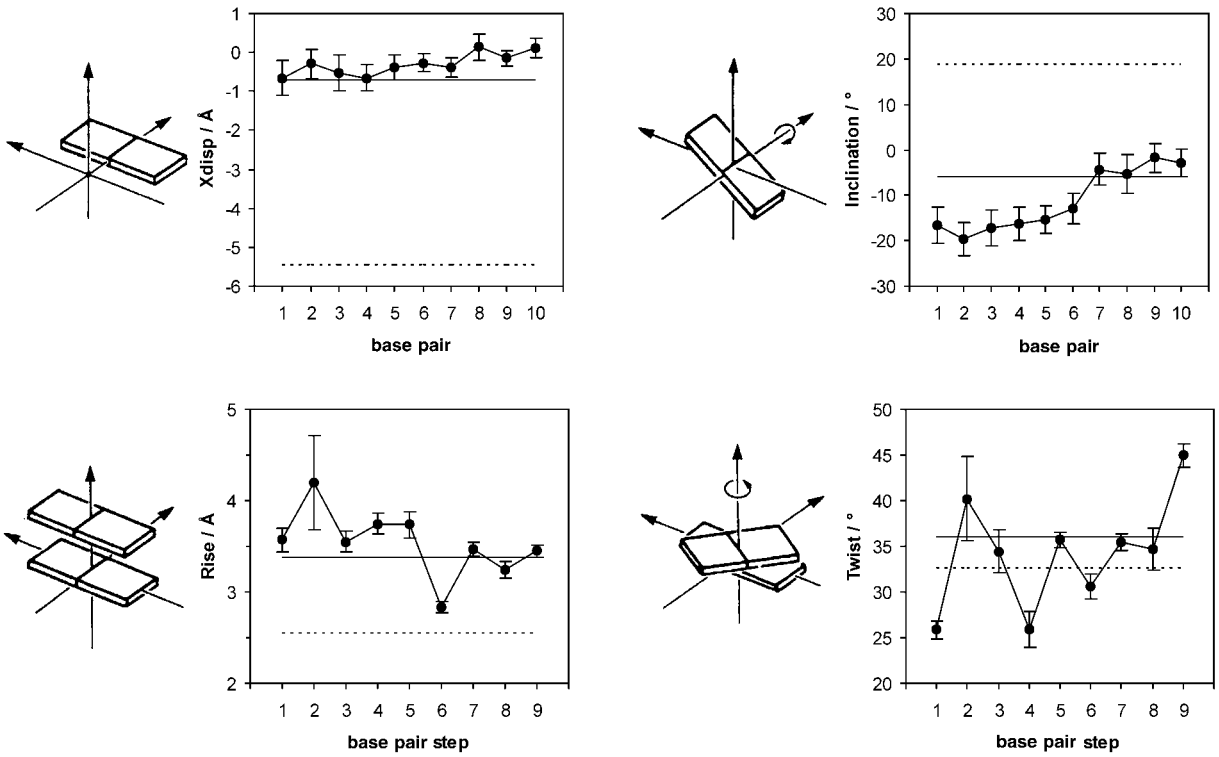

Figure 6. A few of the helicoidal parameters calculated for duplex **1**. The parameters were calculated using CURVES5.2 and are compared to values of canonical A-type duplex (----) and B-type duplex (——) parameters.

Backbone geometry: Due to the intrinsic paucity of NOE restraints in the DNA sugar-phosphate backbone, the backbone geometry of the duplex is less precisely determined than the geometry of the nucleobases in the model structure. Rather, the backbone geometry is determined by the force field employed and by the constraints imposed by the placement of the nucleobases, for stacking and base pairing, and the sugars. However, due to the unusual geometry of the α-L-LNA nucleotides, we think that a general discussion of the salient features of the backbone geometry is of interest.

The backbone angles in the unmodified DNA strand do not differ significantly from normal B-type DNA values, but significant changes are observed in the modified α-L-LNA strand as a consequence of the rearrangement of malleable DNA backbone in order to accommodate the modified nucleotides. The backbone angles of the α-L-LNA strand in the model structure is given in Table 6. The α-L-LNA nucleotides adopt two diverse backbone conformations, in which nucleotides 2 and 5, and 6 and 8, respectively, are paired together. Common to both conformations is that the change in the δ angle brought about by the L-configuration of α-L-LNA is counteracted by changes in the γ- and ζ-angles. The backbone conformation that is adopted by nucleotides 2 and 5 is identical to the conformation that we found in the α-L-LNA nucleotides in an MD simulation of a partly modified α-L-LNA:RNA hybrid.[26]

Table 6. Backbone angles in the α-L-LNA strand in the model structure of duplex **1**.

		α-L-LNA Nucleotides	
	deoxyriboses	T2 and T5	T6 and T8
α	g−	g−	t
β	t	t	t
γ	g+	t	t
δ	g+[a]	g−	g−
ε	t	t	g+
ζ	g−	g+	g+

[a] Approximately 110°.

The glycosidic angles, χ, are found in *anti* conformations for all nucleotides as expected from the NOESY spectra. However, the values differ between deoxyriboses and α-L-LNA nucleotides, the deoxyriboses having an average value of ≈ −120° and the α-L-LNAs an average of ≈ −160°. In our previous MD simulation of an α-L-LNA:RNA hybrid, we also found glycosidic angles of ≈ −160° for the α-L-LNA nucleotides. Therefore this glycosidic angle appear to be suitable for presenting the α-L-LNA nucleobases for Watson–Crick base pairing and base stacking.

Sugar conformations: The sugar conformations of the deoxyriboses in the model structure are found in the *S*-type range (≈120° < *P* < ≈160°) with the exception of G9 and C10, the two 3′-terminal nucleotides in the α-L-LNA strand, which adopt somewhat more northern conformations with pseudorotation angles of 63 and 55°, respectively. The sugar conformations of the model structure are in agreement with the results obtained by analysis of the sugar coupling constants (see above), although some of the pseudorotation values that were measured in the model structure are slightly lower than those determined by coupling constant analysis. This is likely related to the lack of inclusion of dynamics in the NOE derived model structures. The pseudorotation angles of the

  0947-6539/02/0813-3006 $ 20.00+.50/0 *Chem. Eur. J.* **2002**, *8*, No. 13

four α-L-LNA sugars are all near $P = 14°$ (the L-configuration taken into account) and this is consistent with our previous findings.[26]

Discussion

The two α-L-LNA modified duplexes both exhibit NMR spectral features typical of right-handed DNA helices that possess overall B-like geometries with their nucleobases in *anti* conformations and that form normal Watson–Crick base pairs. The B-like appearances of the two duplexes studied are corroborated by the CD spectra displayed in Figure 1.

Comparison of the chemical shift values of the two α-L-LNA modified duplexes with the corresponding values of the unmodified duplexes[14, 15] shows that the most conspicuous differences are the large upfield shifts of the H2 protons of the adenine bases paired with α-L-LNA nucleotides. For duplex **1**, the largest changes are observed for H2 of A13, A16, and A19 with upfield shifts of 0.64, 0.34, and 0.43 ppm, respectively. For duplex **2**, the upfield shifts for A12, A14, and A17 are 0.38, 0.24, and 0.37 ppm, respectively. A similar trend was observed for the adenines that are base-paired to LNA nucleotides in the corresponding LNA modified duplexes, that is the duplexes of identical base that incorporate LNA nucleotides rather than α-L-LNA nucleotides. As the H2 proton of adenine is sited in the centre of the duplex, change in the chemical shift of this proton is an indicator of change in the base-stacking. Indeed, in our model structure of duplex **1**, the H2 protons of A13, A16, and A19 are located above the aromatic planes of purines. In a standard B-type model, these protons would be located on the edge of the aromatic ring system of the purine. A displacement like the one described for the model structure would result in upfield shifts due to the increased ring current effect from neighbouring aromatic rings.

Our analyses of the deoxyribose conformations in both of the α-L-LNA:DNA duplexes show that with the exception of the two 3′-terminal nucleotides in the α-L-LNA strands, all deoxyriboses adopt almost pure *S*-type sugar puckers. This is consistent with the gross B-like duplex appearances as indicated by the NOESY and CD spectra. Thus, the incorporation of the α-L-LNA nucleotides appears to leave the unmodified part of the duplexes unperturbed.

The model structure of duplex **1** possesses the general appearance of a B-type duplex as indicated by base planes almost perpendicular to the helix axis, by a number of the helical parameters, and by sugar conformations in the *S*-range of the pseudorotation cycle. In addition, we find an average minor groove width of 5.7 Å which is typical of a B-type duplex. Thus, the inclusion of four α-L-LNA nucleotides does not perturb the global structure of the duplex. The 2′-*O*,4′-*C* methylene bridges of the α-L-LNA nucleotides are positioned at the brim of the major groove, and fit snugly between their own nucleobases and the 3′-flanking ones, with distances from the 2′-oxygen contacts to these nucleobases that vary between 2.8 and 3.5 Å.

Although the global B-like duplex structure is retained upon introduction of the modified nucleotides, the local structure of the sugar-phosphate backbone is severely perturbed by the L-configured nucleotides and rearranges in their vicinity as shown by Table 6. In our model structure, the four modified nucleotides adopt two diverse backbone conformations with different α and ε angles. Due to the chemical structure of the DNA backbone, it is notoriously difficult to obtain experimental information on the α angle. The $^3J_{H3'P}$ coupling constant yields information on the ε-angle conformation. However, in the case of α-L-LNA, both $\varepsilon = t$ and $\varepsilon = g+$ would yield rather similar $^3J_{H3',P}$ coupling constants ($^3J_{H3',P} \approx 2.5–6$ Hz) and would therefore be of limited value. In native nucleic acids, the $\varepsilon = g+$ conformation is strongly unfavourable due to bad van der Waals contacts between the phosphate group and the sugar ring. This is not the case for α-L-LNA modified nucleic acids, where it is the $\varepsilon = g-$ conformation that is prohibited for steric reasons. It is likely that the α-L-LNA backbone retains the high plasticity of the native DNA backbone, where multiple backbone conformations are energetically allowed. To delineate the intrinsic energetics of different rotamers in the α-L-LNA backbone, further experimental and theoretical studies are needed.

In the model structure, there is a discontinuity in the duplex framework at the $^{\alpha L}$**T**^{L}6pC7:G14pA15 base pairs steps. This interruption is clearly visible in the structure as T6 unstacks from C7, and therefore, T6 stacks with T5 and C7 stacks with T8, and is also evident in a number of the helical parameters. In our high resolution structure of the LNA version of duplex **1**, no such discontinuity was observed in the corresponding base pairs.[14] As such, this anomaly may be an intrinsic property of the preceding α-L-LNA dinucleotide step, although further investigations are required to confirm this. In the base paired DNA strand, the nucleobases stack continuously through the helix, although a kink in the backbone is observed at nucleotide A15.

We have previously performed structural studies of a number of LNA:DNA and LNA:RNA duplexes and have found that LNA nucleotides perturb flanking sugars, particularly the 3′-flanking sugars, towards *N*-type sugar puckers with respect to the unmodified duplexes.[10, 12–16] However, this study and the study of an α-L-LNA:RNA hybrid[26] indicate that the inclusion of α-L-LNA nucleotides does not produce similar conformational steering. Moreover, it can be gauged from the CD spectrum of Figure 1 that the LNA:DNA version of duplex **1** possesses more A-type characteristics than the α-L-LNA:DNA duplex of identical base sequence.

In general, modified nucleic acids that increase helical thermostability are RNA mimics, for example 2′-*O*-alkyl modified RNA,[27] phosphoramidates,[28] and LNA, and hence promote an A-like geometry of the nucleic acid duplex. α-L-LNA, with its unnatural stereochemistry, is a highly unusual nucleic acid analogue, yet α-L-LNA is able to elicit a substantial increase in helical stability when incorporated in native nucleic acid duplexes. How the structural disposition of α-L-LNA translates into an elevated helical thermostability is an intriguing structure–activity problem. Unfortunately, a static structure like our model structure offers no indication of thermodynamic parameters. In addition, a rigorous analysis would require consideration of the single stranded species as well as the duplex. However, the locked nature of the

α-L-LNA nucleotides removes some degrees of freedom in the single stranded α-L-LNA, thus decreasing the entropic gain upon denaturation of an α-L-LNA:DNA duplex relative to a dsDNA duplex. So the introduction of α-L-LNA nucleotides into a dsDNA duplex should entail an entropic gain. The addition of the 2′-oxygens from the α-L-LNAs into the major groove may provide an anchoring point for enhanced solvation of α-L-LNA modified nucleic acids, though such effects are intrinsically difficult to study. From the chemical shifts of the adenine H2 protons, it is evident that the nucleobase stacking is altered in the α-L-LNA modified duplexes with respect to the native dsDNA duplexes, so enhanced stacking interactions may also play a part in the enhanced stability of the modified duplexes.

Conclusion

We have studied two α-L-LNA:DNA duplexes, a nonamer that incorporates three modified nucleotides and a decamer that incorporates four modified nucleotides. Through analyses of the sugar conformations from NMR coupling constants and CD spectroscopy, we have shown that both duplexes adopt general B-like geometries. In addition, we have determined a model structure of the decamer duplex. This structure allows a more detailed picture of the influence exerted by the α-L-LNA nucleotides on the local duplex geometry.

Due to its unnatural stereochemistry, it is futile to compare α-L-LNA with other nucleic acid analogues at the monomeric level or to label the monomer as an "*N*- or *S*-type mimic". However, this study and our previous study of α-L-LNA:RNA hybrids[26] show that when incorporated into duplexes, α-L-LNA acts as a B-type mimic. While the modified DNA duplexes retain their native overall B-type structure, local rearrangements of the sugar-phosphate backbone are shown to be necessary to accommodate the modified nucleotides.

α-L-LNA and LNA are tailored from like bicyclo[2.2.1]-heptane skeletons, and both analogues yield substantial increases in helical thermostability, yet while LNA acts as an A-type mimic, α-L-LNA acts as a B-type mimic.

Experimental Section

Sample preparation: The d(C$^{\alpha L}$T^{L}GC$^{\alpha L}$T^{L}$^{\alpha L}$T^{L}C$^{\alpha L}$T^{L}GC) and d(C$^{\alpha L}$T^{L}-GA$^{\alpha L}$T^{L}A$^{\alpha L}$T^{L}GC) α-L-LNA oligonucleotides were synthesised as described elsewhere.[17, 18] The unmodified complementary oligonucleotides were purchased from DNA Technology, Århus, Denmark. All oligonucleotides were purified by site-exclusion chromatography on a Sephadex G15 column. The two duplexes were obtained by dissolving equimolar amounts of the complementary strands in 10 mM sodium phosphate buffer (pH 7.0), 0.05 mM NaEDTA, 0.01 mM NaN_3, and 0.1 mM sodium 3-(trimethylsilyl)-1-propanesulfonate (DSS) to a volume of 0.5 mL. The mixtures were heated to 80°C and slowly cooled to achieve hybridisation. The numbering schemes used for the duplexes are shown in Scheme 2.

For experiments carried out in D_2O, the solid duplexes were lyophilized three times from D_2O and redissolved in 99.96 % D_2O (Cambridge Isotope Laboratories). A mixture of 90 % H_2O and 10 % D_2O (0.5 mL) was used for experiments examining exchangeable protons. The final concentration of the duplexes were 2 mM.

NMR experiments: NMR experiments were performed on a Varian UNITY 500 spectrometer at 25°C. NOESY spectra of the two duplexes were acquired in D_2O using 1024 complex points in t_2 and spectral widths of 5000 Hz. A total of 512 t_1 experiments, each with 64 scans and a dwell time of 3.955 s between scans, were recorded using the States phase cycling scheme. The residual signal from HOD was removed by low-power presaturation. For duplex **1**, NOESY spectra with mixing times of 200 and 100 ms were acquired, and for the duplex **2**, NOESY spectra with mixing times of 200 and 50 ms were obtained. NOESY spectra in H_2O were acquired using the WATERGATE NOESY pulse sequence for both duplexes with spectral widths of 12000 Hz using 2048 complex points in t_2, 64 scans and a dwell time of 2.171 s between scans. TOCSY spectra with mixing times of 90 ms were obtained in the TPPI mode. In addition, selective DQF-COSY spectra were acquired using a pulse sequence where the first pulse was replaced with an E-BURP type selective pulse[29] in order to enhance the digital resolution in F_1. These spectra were acquired with spectral widths of 5000 Hz in F_2 and 1200 Hz in F_1, respectively, and a total of 500 t_1 experiments, each with 64 scans, with 2048 complex points in t_2.

The acquired data were processed using FELIX (version 97.2, MSI, San Diego, CA). All spectra were apodized by skewed sinebell squared functions in F_1 and F_2.

The H1′ – H2′ and H2″ regions of the DQF-COSY spectra were used as input to CHEOPS[30] to obtain *J* coupling constants for the H1′, H2′, H2″, and H3′ deoxyribose ring protons. The deoxyribose conformations were derived by use of PSEUROT[31] assuming a fast two-state equilibrium between two conformations (*N*- and *S*-type) as previously described.[13]

Model of duplex 1: The upper and lower diagonal parts of the 100 ms NOESY spectrum were integrated separately with FELIX and yielded two peak intensity sets. These sets were used to calculate interproton distance bounds by using the RANDMARDI procedure[32] of the complete relaxation matrix analysis method MARDIGRAS.[33] A total of 165 upper diagonal and 190 lower diagonal NOE cross peak intensities from the NOESY spectrum with a mixing time of 100 ms were included in the RANDMARDI calculations. RANDMARDI returned 178 interproton distances not determined by the covalent geometry. Prior to inclusion in the structure determination, an additional 0.2 Å was added to upper bounds and 0.1 Å was subtracted from lower bounds. The distribution of the interproton distances is shown in Figure 7. Normal Watson – Crick base pairing was inferred from the NOESY spectrum acquired in H_2O and consequently 26 hydrogen bond distance restraints were included with lower and upper bond length bounds of 1.74 Å and 2.10 Å, respectively. An additional 28 distance restraints with loose bonds were obtained from the NOESY spectrum in H_2O. These distance restraints were derived using the isolated spin-pair approximation (ISPA) with cytosine H5 – H6 cross peaks as reference peaks. Due to the inherent error in ISPA and the possibility of exchange of labile protons, wide bounds (ISPA distance ± 1 Å) were set for these restraints. After evaluation of the structures from preliminary restrained molecular dynamics (rMD) calculations, a repulsive restraint between G20 – H4′ and C4 – H4′ was included in the calculations in order to avoid the collapse of this end of the duplex. The inclusion of this restraint is justified as no NOE cross peak is observed between this proton pair. This repulsive restraint had a lower limit of 4.50 Å. In addition, 55 backbone torsion angle restraints were included for the unmodified nucleotides: $-90° < \alpha < -30°$, $-210° < \beta < -150°$, $30° < \gamma < 90°$, $150° < \varepsilon < 210°$, and $-150° < \zeta < -90°$. These values encompass both A- and B-type duplex structures. Four base planarity restraints were included for each of the three terminal base pairs; C1:G20, G9:C12, and C10:G11. For each sugar with almost exclusive *S*-type conformation, which was every sugars except those of the terminal nucleotides G9 and C10 and those of the modified nucleotides T2, T5, T6, and T8, two dihedral angles were included to restrain the deoxyribose: $145° < \tilde{\nu}_{H1',H2'} < 165°$ and $45° < \tilde{\nu}_{H2',H3'} < 25°$.

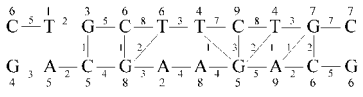

Figure 7. The distribution of NOE restraints obtained from RANDMARDI calculations. The numbers of intra-nucleotide, sequential, and cross-strand restraints are indicated.

0947-6539/02/0813-3008 $ 20.00+.50/0 *Chem. Eur. J.* **2002**, *8*, No. 13

The starting structure for the model refinement was a standard B-form dsDNA duplex built with the *nucgen* and *nukit* modules of AMBER 5.[34] The α-L-LNA nucleotides were added to the B-form duplex using the *xleap* module and atomic charges for the modified nucleotides were calculated using the RESP procedure as described by Bayly et al.[35] A table with atomic charges for α-L-LNA is included as Supporting Information. Initially, the starting structure was restrained energy minimised before being subjected to 28 ps of molecular dynamics in time-steps of 1 fs: 4 ps at 400 K and then cooled to 300 K over 24 ps. Finally, the structure was restrained energy minimised. A distance dependent dielectric constant, $\varepsilon = 4r$, was used and the non-bonded cutoff length was 16 Å. Force constant values of 40 kcal mol^{-1} Å^{-2} were used for distance restraints, 10 kcal mol^{-1} rad^{-2} for backbone angle restraints, 20 kcal mol^{-1} rad^{-2} for the base pair planarity restraints and the dihedral restraints, which were derived from analysis of sugar coupling constants. Finally, the 26 hydrogen-bond restraints were included with force constant values of 40 kcal mol^{-1} Å^{-2}. Due to the paucity of experimental distance restraints in the C1:G20 base pair, this base pair was held fixed during the simulated annealing calculations using the *belly* option of AMBER. This measure ensured suitable convergence of the calculated structural ensemble. During the restrained energy minimisations, the C1:G20 base pair was allowed to move.

Thermal stability studies: The thermal stabilities of duplexes **1** and **2** and the corresponding unmodified dsDNA duplexes were determined spectrophotometrically with a spectrophotometer equipped with a thermoregulated Peltier element. Hybridisation mixtures were prepared by dissolving equimolar amounts (2.5–3.5 μM) of the oligonucleotides in 10 mM sodium phosphate buffer at pH 7.0, 100 mM NaCl, and 0.05 mM EDTA. The absorbance at 260 nm was monitored while the temperature was raised linearly from 10 to 80 °C (1 °C min^{-1}). The melting temperatures, T_m, were obtained as the maxima of the first derivatives of the melting curves.

CD spectra: CD spectra of the α-L-LNA:DNA duplexes from 195 to 360 nm were measured on a Jasco 710/720 spectropolarimeter at 25 °C. Solutions were prepared by dissolving equimolar (40–80 μM) amounts of the oligonucleotides in 10 mM sodium phosphate buffer at pH 7.0, and 0.05 mM EDTA. The spectrum of the buffer solution was subtracted from each spectrum. The molar CD, $\Delta\varepsilon$, of the duplexes was calculated from Equation (1),[36, 37] where θ_{obs} is the measured ellipticity in degrees, L is the path length in cm and c is the concentration of the duplexes.

$$\Delta\varepsilon = \theta_{obs}/(32.98 \times Lc)$$

Absorbance spectra of the solutions were measured on a Lambda 17 spectrophotometer. Concentrations of the duplexes were determined from their absorbance at 260 nm using an extinction coefficient of $\varepsilon = 168\,640$ M^{-1} cm^{-1} for the decamer duplexes and $\varepsilon = 157\,600$ M^{-1} cm^{-1} for the nonamer duplexes.

Protein data bank accession codes: Coordinates and restraints employed in calculations have been deposited in the Protein Data Bank (accession code: 1GV6).

Acknowledgement

We thank the Danish National Research Foundation, The Danish Natural Science Research Foundation, and the Danish Technical Research Foundation for financial support. Britta M. Dahl and Karen Jørgensen (Department of Chemistry, University of Copenhagen) are thanked for oligonucleotide synthesis and for recording the CD spectra, respectively.

[1] S. M. Freier, K. -H. Altmann, *Nucleic Acids Res.* **1997**, *25*, 4429–4443.
[2] A. A. Levin, *Biochem. Biophys. Acta* **1999**, *1489*, 69–84.
[3] W. S. Marshall, M. H. Caruthers, *Science* **1993**, *259*, 1564–1570.
[4] M. J. Damha, C. J. Wilds, A. Noronha, I. Brukner, G. Borkow, D. Arion, M. A. Parniak, *J. Am. Chem. Soc.* **1998**, *120*, 12976–12977.
[5] J. Wang, M. Froeyen, C. Hendrix, G. Andrei, R. Snoeck, E. De Clercq, P. Herdewijn, *J. Med. Chem.* **2000**, *43*, 736–745.
[6] J. Wang, B. Verbeure, I. Luyten, E. Lescrinier, M. Froeyen, C. Hendrix, H. Rosemeyer, F. Seela, A. Van Aerschot, P. Herdewijn, *J. Am. Chem. Soc.* **2000**, *122*, 8595–8602.
[7] A. A. Koshkin, S. K. Singh, P. Nielsen, V. K. Rajwanshi, R. Kumar, M. Meldgaard, C. E. Olsen, J. Wengel, *Tetrahedron* **1998**, *54*, 3607–3630.
[8] S. K. Singh, P. Nielsen, A. A. Koshkin, J. Wengel, *Chem. Commun.* **1998**, 455–456.
[9] S. Obika, D. Nanbu, Y. Hari, J. Andoh, K. Morio, T. Doi, T. Imanishi, *Tetrahedron Lett.* **1998**, *39*, 5401–5404.
[10] K. Bondensgaard, M. Petersen, S. K. Singh, V. K. Rajwanshi, J. Wengel, J. P. Jacobsen, *Chem. Eur. J.* **2000**, *6*, 2687–2695.
[11] C. Wahlestedt, P. Salmi, L. Good, J. Kela, T. Johnsen, T. Hökfelt, C. Broberger, F. Porreca, A. Koshkin, M. H. Jacobsen, J. Wengel, *Proc. Natl. Acad. Sci. USA* **2000**, *97*, 3344–5638.
[12] C. B. Nielsen, S. K. Singh, J. Wengel, J. P. Jacobsen, *J. Biomol. Struc. Dyn.* **1999**, *17*, 175–191.
[13] M. Petersen, C. B. Nielsen, K. E. Nielsen, G. A. Jensen, K. Bondensgaard, S. K. Singh, V. K. Rajwanshi, A. A. Koshkin, B. M. Dahl, J. Wengel, J. P. Jacobsen, *J. Mol. Recognit.* **2000**, *13*, 44–53.
[14] K. E. Nielsen, S. K. Singh, J. Wengel, J. P. Jacobsen, *Bioconjugate Chem.* **2000**, *11*, 228–238.
[15] G. A. Jensen, S. K. Singh, R. Kumar, J. Wengel, J. P. Jacobsen, *J. Chem. Soc. Perkin Trans. 2* **2001**, 1224–1232.
[16] M. Petersen, K. Bondensgaard, J. Wengel, J. P. Jacobsen, *J. Am. Chem. Soc.* **2002**, *124*, in press.
[17] V. K. Rajwanshi, A. E. Håkansson, B. M. Dahl, J. Wengel, *Chem. Commun.* **1999**, 1395–1396.
[18] V. K. Rajwanshi, A. E. Håkansson, R. Kumar, J. Wengel, *Chem. Commun.* **1999**, 2073–2074.
[19] V. K. Rajwanshi, A. E. Håkansson, M. D. Sørensen, S. Pitsch, S. K. Singh, R. Kumar, P. Nielsen, J. Wengel, *Angew. Chem.* **2000**, *112*, 1722–1725; *Angew. Chem. Int. Ed.* **2000**, *39*, 1656–1659.
[20] D. R. Hare, D. E. Wemmer, S. -H. Chou, G. Drobny, B. R. Reid, *J. Mol. Biol.* **1983**, *171*, 319–336.
[21] K. Wüthrich, *NMR of Proteins and Nucleic Acids*, Wiley, New York, **1986**.
[22] J. Feigon, W. Leupin, W. A. Denny, D. R. Kearns, *Biochemistry* **1983**, *22*, 5943–5951.
[23] R. M. Scheek, N. Russo, R. Boelens, R. Kaptein, *J. Am. Chem. Soc.* **1983**, *105*, 2914–2916.
[24] R. Lavery, H. Sklenar, *J. Biomol. Struc. Dyn.* **1988**, *6*, 63–91.
[25] R. Lavery, H. Sklenar, *J. Biomol. Struc. Dyn.* **1989**, *7*, 655–667.
[26] M. Petersen, A. E. Håkansson, J. Wengel, J. P. Jacobsen, *J. Am. Chem. Soc.* **2001**, *123*, 7431–7432.
[27] M. Manoharan, *Biochem. Biophys. Acta* **1999**, *1489*, 117–130.
[28] S. M. Gryaznov, *Biochem. Biophys. Acta* **1999**, *1489*, 131–140.
[29] H. Geen, R. Freeman, *J. Magn. Reson.* **1991**, *93*, 93–141.
[30] R. F. Macaya, P. Schultze, J. Feigon, *J. Am. Chem. Soc.* **1992**, *114*, 781–783.
[31] C. A. G. Haasnoot, F. A. A. M. de Leeuw, C. Altona, *Pseurot 6.2*, *A Program for the Conformational Analysis of Five Membered Rings*, University of Leiden, Leiden, The Netherlands, **1995**.
[32] H. Liu, H. P. Spielmann, N. A. Ulyanov, D. E. Wemmer, T. L. James, *J. Biomol. NMR.* **1995**, *6*, 390–402.
[33] B. A. Borgias, T. L. James, *J. Magn. Reson.* **1990**, *87*, 475–487.
[34] D. A. Case, D. A. Pearlman, J. W. Caldwell, T. E. Cheatham III, W. S. Ross, C. L. Simmerling, T. A. Darden, K. M. Merz, R. V. Stanton, A. L. Cheng, J. J. Vincent, M. Crowley, D. M. Ferguson, R. J. Radmer, G. L. Seibel, U. C. Singh, P. K. Weiner, P. A. Kollman, *AMBER 5*, University of California, San Francisco, **1997**.
[35] C. I. Bayly, P. Cieplak, W. D. Cornell, P. A. Kollman, *J. Phys. Chem.* **1993**, *97*, 10269–10280.
[36] W. A. Baase, W. C. Johnson, *Nucleic Acid Res.* **1979**, *6*, 797–814.
[37] R. W. Woody, *Methods Enzymol.* **1995**, *246*, 34–71.

Received: December 7, 2001 [F3730]